Electronic structure of gold, aluminum, and gallium superatom complexes

O. Lopez-Acevedo,[1,*] P. A. Clayborne,[1] and H. Häkkinen[1,2]
[1]*Nanoscience Center, Department of Chemistry, University of Jyväskylä, 40014 Jyväskylä, Finland*
[2]*Nanoscience Center, Department of Physics, University of Jyväskylä, 40014 Jyväskylä, Finland*
(Received 20 April 2011; published 25 July 2011)

Using *ab initio* computational techniques on crystal determined clusters, we report on the similarities and differences of $Al_{50}(C_5(CH_3)_5)_{12}$, $Ga_{23}(N(Si(CH_3)_3)_2)_{11}$, and $Au_{102}(SC_7O_2H_5)_{44}$ ligand-protected clusters. Each of the ligand-protected clusters in this study shows a similar stable character which can be described via an electronic shell model. We show here that the same type of analysis leads consistently to derivation of a superatomic electronic counting rule, independently of the metal and ligand compositions. One can define the cluster core as the set of atoms where delocalized single-angular-momentum-character orbitals have high weights using a combination of Bader analysis and evaluation of Khon-Sham orbitals. Subsequently, one can derive the nature of the ligand-core interaction. These results yield further insight into the superatom analogy for the class of ligand-protected metal clusters.

DOI: 10.1103/PhysRevB.84.035434 PACS number(s): 73.22.−f, 36.40.−c, 61.46.−w

I. INTRODUCTION

Protected gold clusters have been synthesized in several sizes and compositions. Due to their intrinsic stability and potential applications in nanotechnology, they have received broad interest in past decades. For example, size-dependent optical, electrochemical, and catalytical properties have been experimentally determined.[1–8] In addition, these clusters can be expected to be organized as building blocks of materials with new interesting properties. Recent breakthroughs, such as determination of the crystal structure of ligand-protected clusters,[9–13] have led to further investigations of their electronic structure via *ab initio* simulations. As a result, the electronic structure and derived properties of ligand-protected gold clusters can be modeled via a modified electronic shell model, termed the superatom model.[14–17]

Electronic shell models have been successfully used to understand and predict properties of bare metallic clusters.[18–20] One possible spherical shell model is a three-dimensional (3D) harmonic oscillator with an anharmonic, angular-momentum-dependent, term. From this model several properties are derived, most notably the high stability of some clusters. For a given composition, the model predicts stable clusters with large HOMO-LUMO gaps corresponding to the closing of an electronic shell level. The order of the shells and the magic numbers in this spherical shell model then depend on the anharmonic parameter. For an anharmonic parameter in the intermediate region the order of the shells is

$$1S^2 1P^6 1D^{10} 2S^2 1F^{14} 2P^6 1G^{18} 2D^{10} 3S^2 1H^{22} 2F^{14} 3P^6 1I^{26} 2G^{18},$$

predicting magic numbers at 58 and 138 electrons, among others, corresponding to the closing of the $1G$ and $1I$ shells, respectively ($U = 0.03$; Eq. A_1 from Ref. 20).

Aluminum and gallium metalloid clusters (clusters containing more metal-metal bonds than metal-ligand bonds) have also been characterized experimentally and theoretically in an effort to understand how properties evolve from clusters to bulk and their stability has been explained through various models.[21–23] However, reports on bare aluminum clusters have shown that the most stable species have a superatomic character with a magic number of electrons, which adheres to the electronic shell model.[24,25] For example, the Al_{13}^- cluster is resistive to O_2 etching with 40 electrons (magic number), while its neutral counterpart (Al_{13}) is defined as a superhalogen based on its similar electron affinity to halogens in the periodic table.[24,26–29] This result, along with the studies on ligand-protected gold clusters, suggests that the electronic shell model could describe metalloid clusters composed of aluminum and gallium. Recently our group has analyzed aluminum metalloids and successfully illustrated that a superatom electronic structure exists which relates to a cluster's overall stability.[30] For a few gallium metalloid clusters, it has been predicted that the electronic shell model may be successful; however, to our knowledge, no theoretical investigations into the electronic structure have been performed.

In order to derive an electronic shell structure for nearly spherical ligand-protected clusters, we currently use an orbital projection on spherical harmonics integrated in the cluster region.[14] The orbitals can be labeled with a given angular momentum using the coefficients and one can determine the order of electronic shells in the cluster system. It is necessary, however, to take the role of the ligand layer into account to determine the expected number of delocalized orbitals participating in the shell structure. In the superatom model, one takes the ligand-core interaction into account. In a ligand-protected superatom cluster the core atoms participate collectively to give rise to delocalized orbitals, while the protective units participate only in localized or interface bonding states. The protective ligands can behave by either depleting or donating electrons (or remaining neutral) to the superatom electronic structure and, subsequently, will give rise to different electron counts i.e., magic numbers. The core-ligand interaction not only is important from a theoretical perspective but also proves to have implications in experimental observations.[17,31]

Completing the characterization of the clusters as ligand-protected superatoms requires an understanding of not only the electronic structure, but also the ligand-core interaction. We show, using *ab initio* computational techniques, that three ligand-protected clusters [$Al_{50}Cp^*_{12}Cp^* = C_5(CH_3)_5$, $Ga_{23}L_{11}$, $L = N(Si(CH_3)_3)_2$, and $Au_{102}(SR)_{44}$, $R = C_7O_2H_5$)] can be fully characterized as superatoms. Projection of the

 ©2011 American Physical Society

Kohn-Sham (KS) orbitals on a local atomic basis is used to determine which atomic layers contribute to formation of the delocalized orbitals and are part of the cluster core. Using Bader analysis we find that one can characterize the local atomic electronic structure and gain information on the nature and description of the ligand-protecting shell for each cluster. Based on these analyses of $M_N[X_Y]^z$ clusters, one can predict the number of delocalized electrons using the equation

$$n_e^* = NV_M - YV_X - z, \tag{1}$$

where N is the number of atoms in the core with valence V_M, Y is the number of protective units depleting V_X electrons each, and the cluster has an overall charge of z, that contribute to the superatomic orbitals in the superatom model. Finally, we compare the similarities and differences of the three superatom complexes and their expected properties.

II. COMPUTATIONAL METHODS

The computations were done using the GPAW, which performs calculations based on density functional theory.[32,33] The code is a grid-based implementation of the projector-augmented wave (PAW) method. Furthermore, a frozen core approximation is used. H(1s), C(2s2p), Al(3s3p), S(3s3p), O(2s2p), Au(5d1s), N(2s,2p), Si(3s,3p), and Ga(4s,4p) are treated in the valence. The exchange-correlation functional used in all calculations is PBE.[34] Relaxation of the system is performed until the forces around all atoms are below 0.05 eV/Å. The crystal structures for the $Au_{102}(SR)_{44}$, $Al_{50}Cp^*_{12}$, and $Ga_{23}L_{11}$ were obtained from the experimentally reported structures through the CCDC database.[9,35,36] From the crystal structure the coordinates of a single cluster were isolated and were allowed "in vacuum" to optimize without constraints.

The atomic charge state (extra or missing local charge with respect to the atomic number) is determined using a Bader type of analysis.[37,38] Projecting the all electron partial waves (i.e., the wave functions of the isolated atoms) into molecular orbitals (PLDOS) is done within the PAW formalism following Ref. 33.

The superatomic analysis is done by a projection of the KS orbitals on spherical harmonics.[14] For simplicity, the origin is chosen in the center of mass of the cluster. For a given core radius R_0, the angular momentum weight c_l associated with the KS orbital ψ is defined using

$$c_l = \sum_{m=-l}^{l} f_l^m, \tag{2}$$

$$f_l^m = \int_0^{R_0} \left| \int_\Omega Y_l^{m*}(\theta,\varphi)\psi(r,\theta,\varphi)d\Omega \right|^2 r^2 dr, \tag{3}$$

where $Y_l^m(\theta,\varphi)$ is a spherical harmonic function with degree l and order m, and $d\Omega = \sin\theta d\varphi d\theta$.

III. RESULTS AND DISCUSSION

A. Protected gold clusters, $Au_{102}(SR)_{44}$

First, it is important to see, in the protected gold cluster, that the gold atoms can be divided into two sets: the core and the ligand set.[39] As this result has been derived previously and generalized to other protected gold clusters, we include here the discussion for completeness and as an illustration of the method that will be utilized in the aluminum and gallium case. The $Au_{102}(SR)_{44}$ cluster can be viewed in subsequent layers [Fig. 1(a)]. We find from the analysis that the atoms in the first three layers, r_1 to r_3, each have a very small average Bader charge: 0.01, 0.00, and 0.06 $|e|$, respectively in Fig. 2(a). The atoms in the outermost layer r_4 show a small but distinct positive 0.13 $|e|$ mean charge. The projection on an atomic basis for the inner gold atoms (layers r_1 to r_3) shows an s-p hybrid band with high weights around the highest occupied molecular orbital (HOMO) in the PLDOS [Fig. 3(a)]. In contrast, there is almost no weight on the orbitals around HOMO in the external layer r_4. Those KS orbitals, which also have a high s-p atomic local component, are delocalized superatom orbitals. The superatomic projection shows a change of angular momentum G to H and corresponds to a clear gap of 0.48 between the HOMO and the lowest unoccupied molecular orbital (LUMO)[14] [see Fig. 4(a)]. As a consequence, the superatom core is composed of the first three shells, r_1 to r_3, only, with the core being covered by 21 units $(Au(SR)_2)_{19}$ and $(Au_2(SR)_3)_2$ including the gold atoms belonging to the shell r_4. One can then rewrite the cluster formula, making explicit the core-ligand structure as follows: $Au_{79}[(Au(SR)_2)_{19}(Au_2(SR)_3)_2]$ implies that 79 gold atoms contribute one electron (6s) to the delocalized superatom counting, but 21 of these are depleted by the protective units. This gives that there are 58 superatom electrons, corresponding to a cluster with an electronic closed shell configuration in a spherical potential.

B. Protected aluminum, $Al_{50}(Cp^*)_{12}$

The aluminum metalloid cluster can be viewed geometrically as three distinct shells of aluminum atoms, an inner Al_8 layer, encapsulated by 30 Al atoms, with an exterior shell of 12 Al atoms [Fig. 1(b)]. The exterior 12 aluminum atoms are bonded to 12 pentamethylcyclopentadienyl (Cp^*) ligands. It should be noted that whether the exterior layer should be considered part of the ligand or the core is currently a subject of discussion.[23,40] In order to understand whether or not the outer 12 aluminum atoms are part of the ligand, we performed a similar *ab initio* simulation analysis to determine the core and ligand sets as well as the electronic state of the atoms.

The 12 exterior Al atoms have an average Bader charge of 0.91 $|e|$ [Fig. 2(b)], while the innermost atom has a 0 or negative charge. Thus, these 12 Al atoms donate one electron to the electron-withdrawing ligand Cp^*. The projection of KS orbitals on a local atomic basis is described in Fig. 3(b), where it is shown that all shells, r_1 to r_3, contribute to the delocalized superatomic orbitals. The outermost shell, r_3, near the HOMO level shows more s states than p per atom, which can be attributed to the loss of 1 p electron per Al atom and corresponds to the Bader charge results. Further, the projection on spherical harmonics shows that the $Al_{50}(Cp^*)_{12}$ has an electronic structure corresponding to the one expected for a superatom cluster with a shell closing of 138 electrons as reported previously[30] [see Fig. 4(b)]. The HOMO-LUMO gap (0.94 eV) corresponds to the transition from the 1I shell

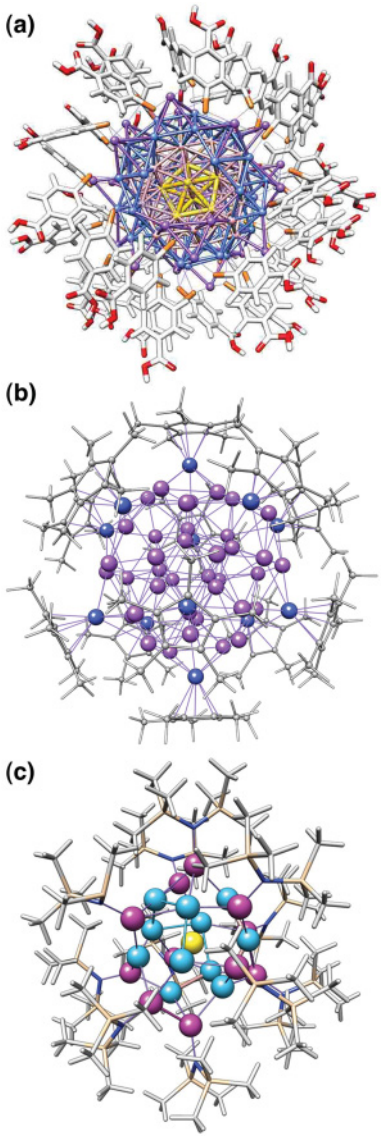

FIG. 1. (Color online) Radial atomic decomposition of ligand-protected clusters considered. Metal atoms are represented by spheres and all others by sticks. Metal atoms in the same radial layer share the same color. Some atoms have been removed to enhance the view of the core. (a) Protected gold cluster, $Au_{102}(SC_7O_2H_5)_{44}$: r_1, r_2, r_3, and r_4 are shown in yellow, pink, blue, and violet, respectively. (b) Protected aluminum cluster, $Al_{50}(C_5(CH_3)_5)_{12}$: r_1 and r_2 are shown in violet and r_3 in blue. (c) Protected gallium cluster, $Ga_{23}(N(Si(CH_3)_3)_2)_{11}$: r_1, r_2, and r_3 are shown in yellow, blue, and violet, respectively.

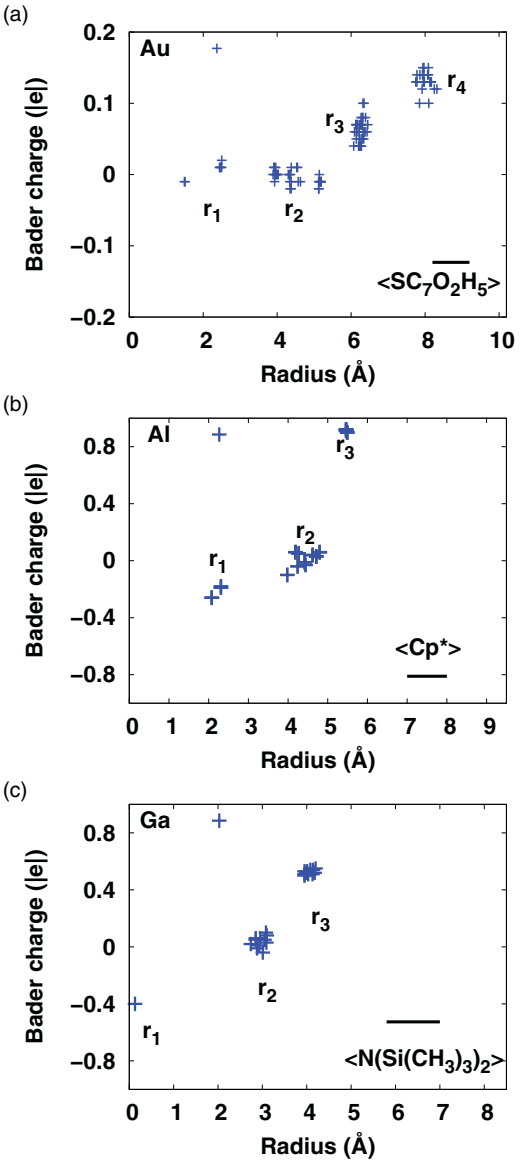

FIG. 2. (Color online) Bader charge as a function of the radial position of atoms. Negative charge indicates excess with respect to the neutral atom charge. The origin of the coordinates is chosen in the center of mass of the cluster. Metal atoms are all included individually. The rest of the charge is indicated as a per ligand average. (a) Protected gold cluster, $Au_{102}(SC_7O_2H_5)_{44}$. (b) Protected aluminum cluster, $Al_{50}(C_5(CH_3)_5)_{12}$. (c) Protected gallium cluster, $Ga_{23}(N(Si(CH_3)_3)_2)_{11}$.

to the 2G shell. The splitting of those 1I and 2G shells can be obtained within the spherical shell model with the anharmonic parameter indicated in the Introduction (Sec. I). Further, when changing the radius parameter in the projection of spherical harmonics, we confirm that it is important to include the most outer aluminum atoms since they contribute to form the higher delocalized superatomic orbitals (Fig. 1 in Supplemental Material).[41] Thus, the combination of these results points to the characterization of this metalloid cluster as a ligand-protected superatom with ionic bonding to Cp* ligands. The structural separation in the core-ligand can be represented by writing the chemical formula as $Al_{50}[Cp^*_{12}]$. The 50 Al atoms of the core contribute three electrons each, while each protective ligand Cp* depletes one electron, giving a total number of 138 superatom electrons.

C. Protected gallium, $Ga_{23}R_{11}$

The $Ga_{23}(N(SiMe_3)_2)_{11}$ metalloid cluster can also be viewed as a cluster containing multiple radial atomic layers as in the previous two cases [Fig. 1(c)]. The innermost layer consists of 1 gallium atom, followed by two consecutive layers of 11 gallium atoms, with the outer 11 being surrounded by ligands. Previously, the gallium metalloid cluster has been described as a Ga_{12} core surrounded by 11 GaL units.[35]

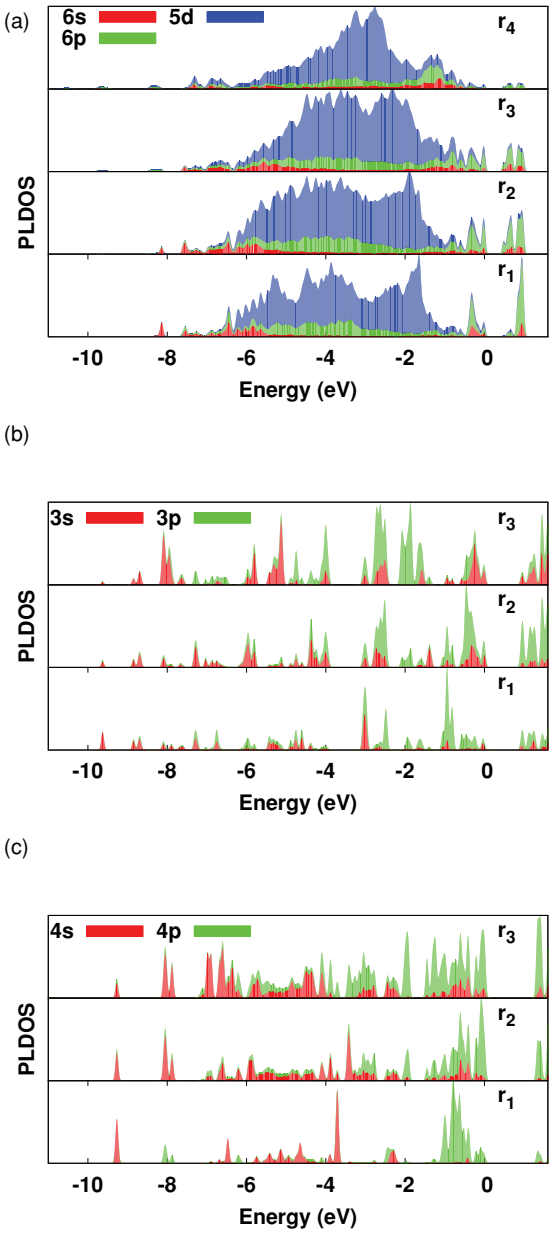

FIG. 3. (Color online) Projected local density of states using atomic basis. The projection is integrated in the radial layers composed by metal atoms. (a) Protected gold cluster, $Au_{102}(SC_7O_2H_5)_{44}$. (b) Protected aluminum cluster, $Al_{50}(C_5(CH_3)_5)_{12}$. (c) Protected gallium cluster, $Ga_{23}(N(Si(CH_3)_3)_2)_{11}$.

We find that the 11 Ga atoms on the exterior layer have an average Bader charge of 0.52 $|e|$, with the inner shell having a negative, -0.40 and a neutral 0.04 $|e|$ mean Bader charge [Fig. 2(c)]. The Bader charge value is indicative of polarized bonding, which should come as no surprise since the ligand is composed of nitrogen. It is well known that nitrogen atoms participate in polarized bonding. From the projection on a local atomic basis, PLDOS [Fig. 3(c)], it is obtained that all gallium atoms are in the same electronic state and contribute to the delocalized superatom states around HOMO. The combination of Bader analysis and PLDOS allows us to conclude that the gallium cluster should be described as a metallic core of 23 atoms protected by 11 electron depleting units. The

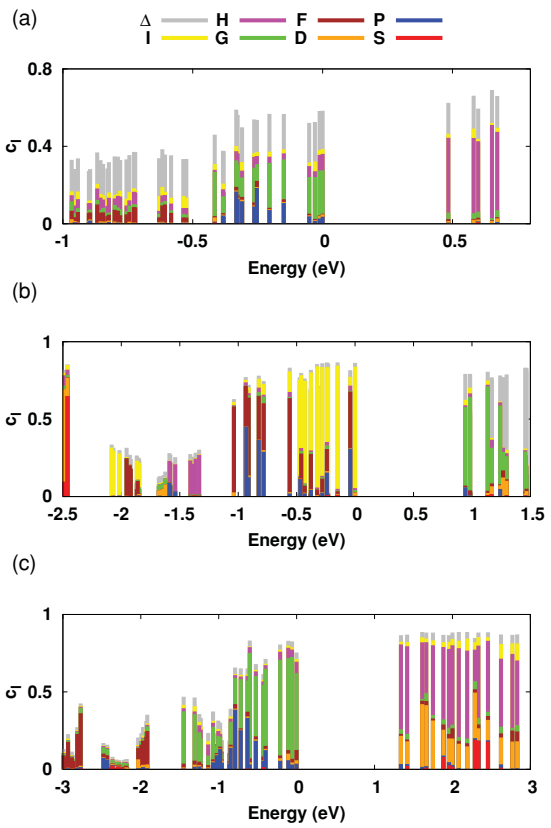

FIG. 4. (Color online) Superatom analysis: angular momentum coefficient c_l from Eq. (2) ($l = 0,1,\ldots,6$) as a function of the energy of the projected KS orbital. The difference between the sum of the coefficients and the norm of the KS orbital inside the sphere of radius R_0 is Δ. (a) Protected gold cluster, $Au_{102}(SC_7O_2H_5)_{44}$; the value of R_0 is 7.5 Å. (b) Protected aluminum cluster, $Al_{50}(C_5(CH_3)_5)_{12}$; the value of R_0 is 6 Å. (c) Protected gallium cluster, $Ga_{23}(N(Si(CH_3)_3)_2)_{11}$; the value of R_0 is 5.5 Å.

projection of the KS orbitals on spherical harmonics reveals that the ligand-protected gallium cluster does adhere to the superatom model with a closed 1G shell with 58 superatomic electrons [Fig. 4(c)]. The cluster has a large gap of 1.34 eV, which is indicative of its stable nature as well. The derived core-ligand composition is thus $Ga_{23}[R_{11}]$, with 23 gallium atoms contributing 3 electrons each and 11 protective units depleting 1 electron, hence corresponding to a counting of 58 superatom electrons.

D. Comparison

All three clusters considered in this study have a core that can be separated into concentric layers, with each layer being formed by metal atoms having not only the same radius but also the same local Bader charge. Likewise, their electronic

TABLE I. Formulas and derived superatomic counting rule.

$M_N[X_Y]^z$	$n_e = NV_M - YV_X - z$
$Au_{79}[(Au(SR)_2)_{19}(Au_2(SR)_3)_2]$	$n_e = 79 - 21 = 58$
$Al_{50}[Cp^*_{12}]$	$n_e = 3 \times 50 - 12 = 138$
$Ga_{23}[R_{11}]$	$n_e = 3 \times 23 - 11 = 58$

structure can be explained using the superatom model, with the number of electrons contributing to the delocalized superatomic orbitals obtained using Eq. (1). Using this electron counting rule, one obtains 58, 138, and 58 electrons for the $Au_{102}(SR)_{44}$, $Al_{50}Cp^*_{12}$, and $Ga_{23}(N(SiMe_3)_2)_{11}$ clusters, respectively (see Table I). Each of the clusters are superatom complexes, but the projection on the local atomic basis shows differences in the layers that contribute to the delocalized superatomic orbitals. For the gold cluster, the gold atoms in the protective exterior do not participate to form such orbitals. In the case of metalloid superatom complexes, their exterior metal atoms do contribute to form superatomic orbitals. Further differences can be seen from the Bader analysis. The charge distribution in the ligand-protected aluminum and gallium clusters proceeds from negative to neutral to positive from the center to the outer shells. However, in the ligand-protected gold cluster the innermost two shells (r_1 and r_2) are neutral, with the third shell, r_3, being only slightly positive and the exterior shell, r_4, being positive as well. Another difference is found when focusing on the ligand and exterior atomic layer interaction. The exterior metal atoms in all three cases have very different Bader values, with the aluminum value being the largest (0.91 $|e|$) and the gold value the smallest. It is interesting that the gallium value is 0.52 $|e|$, yet still positive, as for both aluminum and gold. These differences point to the nature of the ligand-metal bonding in the superatom complexes. It is well known that the bonding for many ligand-protected gold clusters is covalent. We have shown that one can have ionic and polarized covalent bonding in other superatom complexes as seen in the aluminum and gallium cases presented here.

IV. CONCLUSION

We have investigated three distinct ligand-protected clusters composed of gold, aluminum, and gallium. The electronic structure of these clusters can be described via the superatom model and have magic numbers corresponding to 58, 138, and 58 electrons, respectively. One can also define the metallic core as the group of atoms which participate in the delocalized superatomic orbitals using the analyses presented here. Finally, we present evidence that the charge distribution in the core varies strongly with the clusters and does not affect the validity of the electronic shell model. The charge variation is related to the metal-ligand bonding, which also varies with the clusters. We found a covalent, ionic, and polarized covalent bond for the $Au_{102}(SR)_{44}$, $Al_{50}Cp^*_{12}$, and $Ga_{23}L_{11}$ clusters, respectively. As previously done successfully for ligand-protected gold clusters, consequences for optical and charging properties, voltammetry, NMR experiments, and reactivity should be expected for both aluminum and gallium superatom complexes (as well as other compositions). We hope that this study will lead to further theoretical and experimental investigations.

ACKNOWLEDGMENTS

We gratefully acknowledge the Academy of Finland for financial support; CSC, the Finnish IT Center for Science, in Espoo for computational resources; and H.Grönbeck and R. L. Whetten for discussions.

*Corresponding author: lopez@cc.jyu.fi

[1] S. W. Chen, R. S. Ingram, M. J. Hostetler, J. J. Pietron, R. W. Murray, T. G. Schaaff, J. T. Khoury, M. M. Alvarez, and R. L. Whetten, Science **280**, 2098 (1998).
[2] T. G. Schaaff and R. L. Whetten, J. Phys. Chem. B **104**, 2630 (2000).
[3] Y. Negishi, K. Nobusada, and T. Tsukuda, J. Am. Chem. Soc. **127**, 5261 (2005).
[4] N. K. Chaki, Y. Negishi, H. Tsunoyama, Y. Shichibu, and T. Tsukuda, J. Am. Chem. Soc. **130**, 8608 (2008).
[5] M. Brust, M. Walker, D. Bethell, D. J. Schiffrin, and R. Whyman, J. Chem. Soc. Chem. Commun. 1994, 801.
[6] H. Häkkinen, Chem. Soc. Rev. **37**, 1847 (2008).
[7] R. Sardar, A. M. Funston, P. Mulvaney, and R. W. Murray, Langmuir **25**, 13840 (2009).
[8] R. C. Jin, Nanoscale **2**, 343 (2010).
[9] P. D. Jadzinsky, G. Calero, C. J. Ackerson, D. A. Bushnell, and R. D. Kornberg, Science **318**, 430 (2007).
[10] M. W. Heaven, A. Dass, P. S. White, K. M. Holt, and R. W. Murray, J. Am. Chem. Soc. **130**, 3754 (2008).
[11] M. Zhu, C. M. Aikens, F. J. Hollander, G. C. Schatz, and R. Jin, J. Am. Chem. Soc. **130**, 5883 (2008).
[12] C. Femoni, M. C. Iapalucci, G. Longoni, C. Tiozzo, and S. Zacchini, Angew. Chem. Int. Ed. **47**, 6666 (2008).
[13] H. Qian, W. T. Eckenhoff, Y. Zhu, T. Pintauer, and R. Jin, J. Am. Chem. Soc. **132**, 8280 (2010).
[14] M. Walter, J. Akola, O. Lopez-Acevedo, P. D. Jadzinsky, G. Calero, C. J. Ackerson, R. L. Whetten, H. Grönbeck, and H. Häkkinen, Proc. Natl. Acad. Sci. USA **105**, 9157 (2008).
[15] J. Akola, M. Walter, R. L. Whetten, H. Häkkinen, and H. Grönbeck, J. Am. Chem. Soc. **130**, 3756 (2008).
[16] O. Lopez-Acevedo, J. Rintala, S. Virtanen, C. Femoni, C. Tiozzo, H. Grönbeck, M. Pettersson, and H. Häkkinen, J. Am. Chem. Soc. **131**, 12573 (2009).
[17] O. Lopez-Acevedo, H. Tsunoyama, T. Tsukuda, H. Häkkinen, and C. Aikens, J. Am. Chem. Soc. **132**, 8210 (2010).
[18] W. D. Knight, K. Clemenger, W. A. de Heer, W. A. Saunders, M. Y. Chou, and M. L. Cohen, Phys. Rev. Lett. **52**, 2141 (1984).
[19] K. Clemenger, Phys. Rev. B **32**, 1359 (1985).
[20] W. de Heer, Rev. Mod. Phys. **65**, 611 (1993).
[21] K. Wade, Inorg. Nuclear Chem. Lett. **8**, 559 (1972).
[22] D. M. P. Mingos, Acc. Chem. Res. **17**, 311 (1984).
[23] H. Schnöckel, Chem. Rev. **110**, 4125 (2010).
[24] R. E. Leuchtner, A. C. Harms, and A. W. Castleman, J. Chem. Phys. **91**, 2753 (1989).
[25] A. W. Castleman and S. N. Khanna, J. Phys. Chem. C **113**, 2664 (2009).
[26] D. E. Bergeron, A. W. Castleman, T. Morisato, and S. N. Khanna, Science **304**, 84 (2004).
[27] D. E. Bergeron, P. J. Roach, A. W. Castleman, N. Jones, and S. N. Khanna, Science **307**, 231 (2005).

[28] J. U. Reveles, S. N. Khanna, P. J. Roach, and A. W. Castleman, Proc. Natl. Acad. Sci. USA **103**, 18405 (2006).
[29] A. C. Reber, S. N. Khanna, P. J. Roach, W. H. Woodward, and A. W. Castleman, J. Am. Chem. Soc. **129**, 16098 (2007).
[30] P. A. Clayborne, O. Lopez-Acevedo, R. L. Whetten, H. Grönbeck, and H. Häkkinen, Eur. J. Inor. Chem. Issue **2011**, 2649 (2011).
[31] M. Strange, O. Lopez-Acevedo, and H. Häkkinen, J. Phys. Chem. Lett. **1**, 1528 (2010).
[32] W. Kohn and L. J. Sham, Phys. Rev. **140**, 1133 (1965).
[33] J. Enkovaara, C. Rostgaard, J. Mortensen, J. Chen, M. Dulak, L. Ferrighi, J. Gavnholt, C. Glinsvad, V. Haikola, H. Hansen *et al.*, J. Phys. Condens. Matter **22**, 253202 (2010).
[34] J. P. Perdew, K. Burke, and M. Ernzerhof, Phys. Rev. Lett. **77**, 3865 (1996).
[35] J. Hartig, A. Stosser, P. Hauser, and H. Schnöckel, Angew. Chem. Int. Ed. **46**, 1658 (2007).
[36] J. Vollet, R. Burgert, and H. Schnöckel, Angew. Chem. Int. Ed. **44**, 6956 (2005).
[37] R. F. W. Bader, *Atoms in Molecules: A Quantum Theory. International Series of Monographs on Chemistry* (Clarendon Press, Oxford, 1990).
[38] W. Tang, E. Sanville, and G. Henkelman, J. Phys. Condens. Matter **21**(8), 084204 (2009).
[39] H. Häkkinen, M. Walter, and H. Grönbeck, J. Phys. Chem. B **110**, 9927 (2006).
[40] H. Schnöckel, A. Schnepf, R. Whetten, C. Schenk, and P. Henke, Z. Anorg. Allg. Chem. **637**, 15 (2011).
[41] See Supplemental Material at http://link.aps.org/supplemental/10.1103/PhysRevB.84.035434 for a superatomic analysis varying the core radius and tables listing the Bader charges per layer and atoms in the ligand.